European Journal of Pharmaceutics and Biopharmaceutics 79 (2011) 646–657

Contents lists available at ScienceDirect

European Journal of Pharmaceutics and Biopharmaceutics

journal homepage: www.elsevier.com/locate/ejpb

Research paper

Tryptophan-mPEGs: Novel excipients that stabilize salmon calcitonin against aggregation by non-covalent PEGylation

Claudia Mueller [a,b], Martinus A.H. Capelle [c], Tudor Arvinte [a,c], Emek Seyrek [d], Gerrit Borchard [a,b,*]

[a] School of Pharmaceutical Sciences, University of Geneva, University of Lausanne, Geneva, Switzerland
[b] Centre Pharmapeptides, Site d'Archamps, Archamps, France
[c] Therapeomic Inc., Basel, Switzerland
[d] Department of Inorganic, Analytical, and Applied Chemistry, University of Geneva, Geneva, Switzerland

ARTICLE INFO

Article history:
Received 7 October 2010
Accepted in revised form 7 June 2011
Available online 14 June 2011

Keywords:
Protein aggregation
Stability
Salmon calcitonin
Protein formulation
Non-covalent PEGylation

ABSTRACT

Protein aggregation, which is triggered by various factors, is still one of the most prevalent problems encountered during all stages of protein formulation development. In this publication, we present novel excipients, tryptophan-mPEGs (Trp-mPEGs) of 2 and 5 kDa molecular weight and suggest their use in protein formulation. The synthesis and physico-chemical characterization of the excipients are described. Possible cytotoxic and hemolytic activities of the Trp-mPEGs were examined. Turbidity, 90° static light scatter, intrinsic fluorescence, fluorescence after staining the samples with Nile Red and fluorescence microscopy were used to study the inhibitory effect of the Trp-mPEGs on the aggregation of salmon calcitonin (sCT) in different buffer systems and at various molar ratios. Aggregation of sCT was reduced significantly with increasing concentrations of Trp-mPEG 2 kDa. A 10-fold molar excess of Trp-mPEG 2 kDa suppressed almost completely the aggregation of sCT in 10 mM sodium citrate buffer (pH 6) for up to 70 h. Trp-mPEG 5 kDa also reduced the aggregation of sCT, though less pronounced than Trp-mPEG 2 kDa. Low aggregation of sCT was measured after approximately 10 days in 10 mM sodium citrate buffer, pH 5, with a 10-fold molar excess of Trp-mPEG 2 kDa. This paper shows that Trp-mPEGs are potent excipients in reducing the aggregation of sCT. Trp-mPEGs are superior to dansyl-PEGs concerning the stabilization of sCT in a harsh environment, wherein sCT is prone to aggregation. Trp-mPEGs might therefore also be used for stabilization of other biopharmaceuticals prone to aggregation.

1. Introduction

Biologics gained considerably increased market share during the last decade [1–3]. However, chemical and physical degradation, among which aggregation is one of the main concerns, limit the rapid commercialization of protein-based pharmaceuticals [4]. During their manufacturing and formulation processes, proteins are subjected to various stresses, which may lead to aggregation of the biopharmaceutical drug. Processing steps, e.g., freeze drying, pumping, agitation, shear stress, changes in temperature and environmental conditions like buffers, formulation pH or additives, or packaging materials are a few parameters that may affect the stability of a protein [4–6]. Due to the many factors triggering aggregation, and which vary from drug to drug, suppression or reduction in aggregation is most often obtained experimentally by testing various parameters, such as different buffer systems or formulation pH values, under accelerated aggregation conditions [4,7].

For many proteins, aggregation starts by the formation of partially unfolded intermediates. The fraction of unfolded intermediates is usually relatively small but favors protein association, because of an increased amount of exposed hydrophobic patches [8–10]. Native monomers may also aggregate, if 'sticky' patches are present on the protein's surface. Aggregation can then proceed through hydrophobic or electrostatic forces between those patches [9,11].

Covalent conjugation of poly(ethylene glycol), commonly referred to as PEGylation, has been successfully applied to reduce the aggregation of biopharmaceuticals [12–14]. The protective effect of PEG on protein aggregation may be explained by sterical shielding of hydrophobic patches on the protein's surfaces. Further benefits that may be obtained by PEGylation are an increased half-live *in vivo* and a decreased *in vivo* immunogenicity of the biopharmaceutical [15–17]. These positive attributes led to the successful approval of different PEGylated biopharmaceuticals that hold

Abbreviations: Trp, L-tryptophan; Trp-mPEG, tryptophan-mPEG; mPEG, methoxypoly(ethylene glycol); pnp-PEG, *p*-nitrophenyl carbonate mPEG; sCT, salmon calcitonin.

* Corresponding author. School of Pharmaceutical Sciences, University of Geneva, University of Lausanne, 1211 Geneva 4, Switzerland. Tel.: +41 22 379 6945/3802; fax: +41 22 379 6567.
E-mail address: Gerrit.Borchard@unige.ch (G. Borchard).

0939-6411/$ - see front matter © 2011 Elsevier B.V. All rights reserved.
doi:10.1016/j.ejpb.2011.06.003

important therapeutic value in the treatment of severe diseases like cancer (Oncaspar®), hepatitis C (PEGintron®) or severe combined immunodeficiency disease (Adagen®) since the beginning of the 1990s [18].

However, several challenges concerning covalent PEGylation remain, which are (i) the chemical reaction needed in order to attach the PEG-polymer and (ii) the loss of *in vivo* bioactivity observed after PEGylation. Although various techniques have been developed for covalent PEGylation, none has been found that circumvents the chemical reaction and subsequently needed purification. These additional processes during the preparation of the final drug product represent additional stresses for biopharmaceuticals and may lead to aggregation, resulting in a partial or complete loss of *in vivo* bioactivity and increased *in vivo* immunogenicity.

In order to reduce the imposed stresses on biopharmaceuticals during formulation, we presented in a recent publication the new method of stabilization against aggregation by hydrophobic interaction through "non-covalent PEGylation" [19]. The concept is based on non-covalent interaction between the hydrophobic headgroup of a newly synthesized PEG derivative and hydrophobic patches on the surface of biopharmaceuticals. A sterical shielding of the latter by the PEG moiety shall be obtained. Protein/protein interactions should thus be rendered less probable, and consequently aggregation of the biopharmaceutical in liquid formulations should be reduced. A patent application related to this technology has recently been filed [20].

In the previous publication, we were able to show that aggregation of salmon calcitonin (sCT) in liquid formulations was reduced after the addition of dansyl-PEGs of varying molecular weights [19]. In this publication, we present the preparation and physicochemical characterization of PEG conjugates with the amino acid tryptophan (Trp) as hydrophobic headgroup. Although in our studies no hemolysis was observed for both the Trp-PEGs and the dansyl-PEGs, Trp holds the advantage of being used as nutritional supplement for humans [21]. The influence of the monovalent Trp-mPEG polymers of 2 and 5 kDa on the aggregation of sCT was evaluated by performance of accelerated aggregation studies. Trp-mPEGs were superior to dansyl-PEGs in stabilizing sCT against aggregation in a harsh environment, in which sCT in the absence of stabilizing excipients aggregates very fast.

2. Materials and methods

2.1. Materials

The chemicals employed to prepare the buffer solutions, Nile Red (9-diethylamino-5H-benzo[α]phenoxazine-5-one), anhydrous toluene and trifluoroacetic acid (TFA) were supplied by Sigma–Aldrich (Sigma–Aldrich Chemie GmbH, Buchs, Switzerland). The used buffers were constituted of: (i) acetic acid–sodium acetate, pH 5; (ii and iii) citric acid–sodium citrate, pH 5 and pH 6, respectively; (iv) sodium phosphate monobasic–sodium phosphate dibasic, pH 8. Anhydrous DMSO, anhydrous dichloromethane, and L-tryptophan were purchased from Fluka (Sigma–Aldrich Chemie GmbH, Buchs, Switzerland). Chloroform was supplied by Chimie-Plus (Chimie Plus Laboratoires, Denicé, France). Concentrated HCl and anhydrous Na_2SO_4 were obtained from Riedel de Haën (Sigma–Aldrich Laborchemikalien, Seelze, Germany). Diethylether, dichloromethane, anhydrous triethylamine, iso-propanol, and *p*-nitrophenyl chloroformate were provided by Acros (Acros Organics BVBA; Geels, Belgium). The mPEG-OH 2 kDa and 5 kDa were obtained from Iris Biotech (Iris Biotech GmbH, Marktredwitz, Germany). All solvents and compounds used were of analytical grade. The salmon calcitonin was provided by Therapeomic (Therapeomic Inc., Basel, Switzerland). UV transparent 96-well or 384-well Costar® Corning microplates and UV–Vis transparent and pressure sensitive Corning® Universal Optical sealing tape were purchased from Corning (Corning Life Sciences, Schiphol, The Netherlands).

2.2. Characterization of tryptophan-PEGs

All polymers were dissolved in deuterated DMSO and analyzed on a Varian VXR 300 MHz spectrometer (Varian, Switzerland) to obtain ^{1}H NMR and ^{13}C NMR spectra. MALDI-TOF mass spectrometry was performed on an Axima CFR + Shimadzu mass spectrometer, using 2-(4-hydroxyphenylazo)-benzoic acid (HABA) as matrix. A Perkin-Elmer 100 FT-IR spectrometer (Perkin-Elmer, Switzerland) was used to measure FTIR spectra in the range of 4000–400 cm^{-1}. The used pellets were made of 1% w/w of product in KBr. UV spectra were obtained on a Varian Cary 50 spectrophotometer (Varian, Switzerland). The tryptophan-mPEGs were further analyzed for their specific optical rotation properties according to European Pharmacopeia 5.6 using a Perkin-Elmer 241 Polarimeter.

2.3. Synthesis of mPEG-p-nitrophenyl carbonate 2 kDa

The method was adapted from [21]. In short, 1.76 mmol of dried mPEG-OH 2 kDa were dissolved in anhydrous dichloromethane and 5.27 mmol of *p*-nitrophenyl chloroformate and 3.52 mmol of dry triethylamine were added (1:3:2 ratio). The pH was adjusted to a value between 7.5 and 8, and the reaction was left to proceed at room temperature for 24 h. The reaction was stopped by adding several drops of TFA until the solution became colorless; then, dichloromethane was partially evaporated and precipitation from cold diethylether was performed. The solid collected by filtration was twice redissolved in dichloromethane, precipitated from cold diethylether, and collected by filtration. A white powder was obtained and dried under vacuum.

^{1}H NMR (300 MHz, DMSO-d-6): 3.23 ppm, PEG CH_3—O— (s); 3.50 ppm, PEG —O—CH_2— (m); 7.55 ppm, p-nitrophenyl-aromate (d); 8.31 ppm, p-nitrophenyl-aromate (d). ^{13}C NMR (300 MHz, DMSO-d-6): 58.06 ppm, PEG CH_3—O—; 69.52 ppm, PEG —O—CH_2—; 122.59 ppm, p-nitrophenyl-aromate; 125.34 ppm, p-nitrophenyl-aromate; 144.21 ppm, PEG —O—*CH_2*—C=O; 151.99 ppm, aromatic C_5H_4=*C*—NO_2; 155.27 ppm, PEG —CH_2—*OCO*—. FTIR: 3435; 2888; 2739; 2678; 2493; 1967; 1769; 1617; 1594; 1527; 1468; 1360; 1343; 1281; 1242; 1113; 1060; 963; 841; 663; 529 cm^{-1}. MS (MALDI-TOF): *m/z* 2201 (M^+).

2.4. Synthesis of tryptophan-mPEG 2 kDa

The method was adapted from [22]. In anhydrous DMSO, 0.018 mol L-tryptophan was dissolved and the pH was adjusted to a value of ~8.3. Then, 1.76 mmol of dried mPEG-*p*-nitrophenyl carbonate 2 kDa was added. The pH was maintained at a value of approximately 8.3, and the reaction was left to proceed at room temperature for 4 h. The reaction was stopped by cooling to 0 °C and adjusting the pH to a value of 3 with 2 M HCl. The aqueous phase was extracted with chloroform. The obtained organic phase was dried over anhydrous Na_2SO_4 and partially evaporated. Precipitation from cold diethylether was performed and the solid collected by filtration. The solid was once reprecipitated from cold diethylether, and twice from cold iso-propanol. A white powder was obtained and dried under vacuum.

^{1}H NMR (300 MHz, DMSO-d-6): 3.17 ppm, Trp indole—*CH_2*—CH_2— (d); 3.24 ppm, PEG —CH_3—O— (s); 3.51 ppm, PEG —O—CH_2— (m); 4.17 ppm, Trp indole—CH_2—*CH_2*— (q); 6.98 ppm, Trp-indole (t); 7.06 ppm, Trp-indole (t); 7.16 ppm, Trp-indole (s); 7.32 ppm, Trp-indole (d); 7.51 ppm, Trp-indole (d); 10.82 ppm

Trp —COOH (s). ^{13}C NMR (300 MHz, DMSO-d-6): 54.78 ppm, Trp indole—CH_2—*CH_2*—; 58.58 ppm, PEG CH_3—O—; 63.28 ppm, Trp indole—*CH_2*—CH_2—; 69.70 ppm, PEG —O—CH_2—; 110.02 ppm, Trp-indole; 111.33 ppm, Trp-indole; 117.79 ppm, Trp-indole; 120.80 ppm, Trp-indole; 123.65 ppm, Trp-indole; 126.88 ppm Trp-indole; 136.17 ppm, Trp-indole; 156.26 ppm, PEG —CH_2—*OCO*—NH—; 173.87 ppm, —COOH. FTIR: 3412; 2886; 2741; 2695; 2167; 1970; 1721; 1526; 1467; 1413; 1360; 1343; 1280; 1242; 1110; 963; 842; 745, 529 cm^{-1}. MS (MALDI-TOF): *m/z* 2266 (M^+). $[\alpha]_D^{20} = -0.005$.

2.5. Synthesis of mPEG-p-nitrophenyl carbonate 5 kDa

The reaction was performed as described for the mPEG-*p*-nitrophenyl carbonate 2 kDa. In this reaction, 0.68 mMol of dried mPEG-OH 5 kDa, 2.03 mmol of *p*-nitrophenyl chloroformate and 1.36 mmol of dry triethylamine were used, and a white powder was obtained.

^{1}H NMR (300 MHz, DMSO-d-6): 3.23 ppm, PEG CH_3—O— (s); 3.50 ppm, PEG —O—CH_2— (m); 7.55 ppm, p-nitrophenyl-aromate (d); 8.31 ppm, p-nitrophenyl-aromate (d). ^{13}C NMR (300 MHz, DMSO-d-6): 58.27 ppm, PEG CH_3—O—; 69.70 ppm, PEG —O—CH_2—; 122.62 ppm, p-nitrophenyl-aromate; 125.33 ppm, p-nitrophenyl-aromate; 145.93 ppm, PEG —O—*CH_2*—C=O; 152.10 ppm, aromatic C_5H_4=*C*—NO_2; 154.76 ppm, PEG —CH_2—*OCO*—. FTIR: 3447; 2889; 2741; 2694; 2603; 2494; 1971; 1769; 1642; 1526; 1468; 1360; 1343; 1281; 1242; 1219; 1113; 1060; 963; 842; 529 cm^{-1}. MS (MALDI-TOF): *m/z* 4698 (M^+).

2.6. Synthesis of tryptophan-mPEG 5 kDa

The reaction was performed as described for tryptophan-mPEG 2 kDa. In this reaction, 0.68 mmol of dried mPEG-*p*-nitrophenyl carbonate 5 kDa and 6.78 mmol of L-tryptophan were used. A white powder was obtained.

^{1}H NMR (300 MHz, DMSO-d-6): 3.21 ppm, Trp indole—*CH_2*—CH_2— (d); 3.24 ppm, PEG —CH_3—O— (s); 3.51 ppm, PEG —O—CH_2— (m); 4.18 ppm, Trp indole—CH_2—*CH_2*— (q); 6.96 ppm, Trp-indole (t); 7.02 ppm, Trp-indole (t); 7.14 ppm, Trp-indole (s); 7.32 ppm, Trp-indole (d); 7.51 ppm, Trp-indole (d); 10.81 ppm Trp —COOH (s). ^{13}C NMR (300 MHz, DMSO-d-6): 54.85 ppm, Trp indole—CH_2—*CH_2*—; 58.04 ppm, PEG CH_3—O—; 63.46 ppm, Trp indole—*CH_2*—CH_2—; 69.72 ppm, PEG —O—CH_2—; 110.83 ppm, Trp-indole; 111.34 ppm, Trp-indole; 117.99 ppm, Trp-indole; 120.90 ppm, Trp-indole; 124.11 ppm, Trp-indole; 127.04 ppm Trp-indole; 136.62 ppm, Trp-indole; 156.24 ppm, PEG —CH_2—*OCO*—NH—; 173.68 ppm, —COOH. FTIR: 3438; 2885; 2741; 2695; 1969; 1719; 1647; 1467; 1360; 1343; 1281; 1242; 1112; 1060; 963; 842; 746; 529 cm^{-1}. MS (MALDI-TOF): *m/z* 4772 (M^+). $[\alpha]_D^{20} = -0.002$.

2.7. Sensitivity of tryptophan-mPEGs to solvent polarity

In 0%, 25%, 50%, 75% and 100% ethanol, 0.04 mM solutions of tryptophan-mPEGs were prepared. The dielectric constants are 78.54 for water and 24.3 for ethanol 96%. The solutions were analyzed by intrinsic fluorescence and UV–Vis absorbance at 25 °C, using a Fluoromax spectrofluorometer (Spex, Stanmore, UK), and temperature-controlled Cintra 40 spectrophotometer (GBC, Melbourne, Australia), respectively. For tryptophan-mPEG 2 kDa and 5 kDa, the fluorescence emission spectra were recorded between 290 and 450 nm after excitation at 280 nm using bandwidths of 0.3 mm at the excitation and 1 mm at the emission side. The integration time used was 0.01 s.

2.8. Studies of potential of self-association of tryptophan-PEGs

Fluorescence emission of solutions below 0.6 mg/ml and dynamic light scattering at concentrations above 0.1 mg/ml were used to analyze self-association of the Trp-mPEGs. Aqueous polymer solutions of 1 mg/ml were further diluted to obtain solutions at concentrations between 0.6 mg/ml and 0.1 μg/ml, and their fluorescence emission spectra were measured using an excitation wavelength of 280 nm. In order to obtain a sufficiently high fluorescence signal, slit widths were adapted depending on the concentration. Dynamic light scattering (DLS) at an angle of 173° (backscatter) at 25 °C was employed to analyze solutions with concentrations above 0.08 mg/ml by using a Zetaziser Nano ZS (Malvern Instruments), equipped with a 4 mW He–Ne laser that operates at 633 nm. The micellization of Tween 20® was followed as a control experiment for DLS measurements.

2.9. High throughput spectroscopic analysis

The method was adapted from [22]. The four different buffer solutions, (i) 10 mM sodium acetate buffer, pH 5; (ii and iii) 10 mM sodium citrate buffer, pH 5 and 6, respectively; and (iv) 10 mM sodium phosphate, pH 8, were prepared using sterile filtered 100 mM buffer stock solutions. A stock solution of 12.5 mg/ml salmon calcitonin in purified MilliQ™ Millipore water was freshly prepared. The final solutions tested contained 2.5 mg/ml sCT in 10 mM buffer. Each sample was prepared in duplicate and to one of each duplicate, Nile Red (1 μM in final formulation) was added. Each formulation was measured in triplicate. Table 1 shows the different molar ratios and respective concentrations of sCT and Trp-mPEGs.

All sCT solutions were prepared in 96- or 384-well Costar® Corning microplates. Afterward, the plates were sealed using UV–Vis transparent and pressure sensitive Corning® Universal Optical sealing tape.

Every 7.5 min, a cycle of the following was measured at 26 °C with a Tecan Safire™ microplate reader (Tecan Group Ltd., Männedorf, Switzerland): (i) UV–Vis absorbance at 500 nm (turbidity); (ii) fluorescence emission of the hydrophobic dye Nile Red; and (iii) intrinsic Trp fluorescence emission.

The fluorescence emission of Trp over time was determined at 360 nm after excitation at 280 nm using bandwidths of 5 and 12 nm for excitation and emission, respectively. The fluorescence emission of Nile Red was studied over time at 620 nm after excitation at 550 nm using bandwidths of 12 nm for both excitation and emission. After 3 days, the intrinsic Trp fluorescence emission spectra (300–400 nm) and Nile Red fluorescence emission spectra (590–700 nm) were recorded using the same settings as during the kinetics. The data output of the XFluor® software of the Tecan Safire™ microplate reader is in Microsoft® Excel™ format. To facilitate high throughput data analysis, visual basic macros were developed by the authors.

2.10. Interaction of Trp-mPEG 2 kDa with salmon calcitonin (sCT) at different molar ratios in 10 mM sodium citrate buffer, pH 5

2.10.1. Steady-state fluorescence and anisotropy

sCT (12.5 mg/ml) and Trp-mPEG 2 kD (37.17 mg/ml) stock solutions were freshly prepared in 10 mM sodium citrate buffer, pH 5. The tested solutions were (i) 2.5 mg/ml sCT and 18.59 mg/ml Trp-mPEG 2 kDa (1:10 molar ratio protein to excipient), (ii) 2.5 mg/ml sCT and 1.86 mg/ml Trp-mPEG 2 kDa (1:1 molar ratio protein to excipient), and (iii) 2.5 mg/ml sCT in 10 mM sodium citrate buffer, pH 5.

Steady-state fluorescence measurements were performed using a Fluoromax spectrofluorometer (Spex, Stanmore, UK) at 25 °C in a

Table 1
Solutions tested by high throughput spectroscopic analysis. Different molar ratios and the respective concentrations of sCT and Trp-PEGs used.

Sample	Molar ratio	Concentration (mg/ml)
sCT:Tryptophan-mPEG 2 kDa	1:0.5	2.5 mg/ml sCT; 0.93 mg/ml Trp-mPEG 2 kDa
	1:1	2.5 mg/ml sCT; 1.86 mg/ml Trp-mPEG 2 kDa
	1:2	2.5 mg/ml sCT; 3.72 mg/ml Trp-mPEG 2 kDa
	1:5	2.5 mg/ml sCT; 9.29 mg/ml Trp-mPEG 2 kDa
	1:10	2.5 mg/ml sCT; 18.59 mg/ml Trp-mPEG 2 kDa
sCT:Tryptophan-mPEG 5 kDa	1:1	2.5 mg/ml sCT; 4.36 mg/ml Trp-mPEG 5 kDa
	1:5	2.5 mg/ml sCT; 21.79 mg/ml Trp-mPEG 5 kDa

thermostated cuvette holder. The tyrosine fluorescence of sCT was monitored with a 0.01 s integration time at emission wavelengths between 290 and 450 nm, using an excitation wavelength of 275 nm and 280 nm. Bandwidths of 1 mm and 2 mm were used for excitation and emission, respectively, while an optical filter (10% light transmission) was placed at the emission site in front of the detector.

To measure the tryptophan fluorescence, the samples were excited at 295 nm using the same settings and filter arrangement as for tyrosine. Nile Red fluorescence was measured between 590 and 750 nm using an excitation wavelength of 550 nm and slits of 1 mm and 2 mm for excitation and emission, respectively.

Steady-state anisotropy measurements were performed using the above described Fluoromax spectrophotometer with prism polarizers and anisotropy was calculated as described in [24]. The anisotropy value for tyrosine was calculated from fluorescence spectra between 300 and 320 nm, using an excitation wavelength of 275 nm, with one second integration time per 1 nm increment and excitation and emission slits of 1 and 2 mm, respectively. The anisotropy value for Nile Red was calculated from fluorescence spectra between 610 and 630 nm, using an excitation wavelength of 550 nm, with 2 s integration time per 1 nm increment. The excitation and emission slits were 1 and 2 mm, respectively.

2.10.2. 90° light scattering

The intensity of scattered light at a 90° angle was determined as described by Capelle et al. [23] using the Fluoromax spectrofluorometer (Spex, Stanmore, UK). The light scatter was measured between 450 and 700 nm using synchronized excitation and emission monochromators. Slits of 2 mm at the excitation and emission side and an integration time of 0.01 s were used. An optical filter (10% light transmission) was put in front of the detector.

2.10.3. Fluorescence lifetime measurements

Time-correlated single-photon counting (TCSPC) was used to determine fluorescence lifetimes on an IBH 5000U fluorescence lifetime spectrophotometer (Glasgow, United Kingdom) equipped with a 279 nm (Tyr and Trp) or 560 nm (Nile Red) NanoLED as excitation sources and a monochromator at the emission side. Linear and non-linear least-square fittings were performed using DAS6 software (IBH, Glasgow, United Kingdom) to analyze the data. The average lifetimes were calculated using the equation given in [25]:

$$\overline{\tau} = \frac{\sum_i \alpha_i \tau_i^2}{\sum_i \alpha_i \tau_i}$$

where $\overline{\tau}$ is the calculated fluorescence decay time and α the pre-exponential factor.

2.10.4. UV–Vis measurements

UV–Vis absorbance was measured at 25 °C on a Cintra 40 UV–Vis spectrophotometer (GBC, Melbourne) equipped with a thermostatted cuvette holder.

2.10.5. Brightfield and fluorescence microscopy

Aliquots of the samples were placed on Kova Glasstic slides (Hycor, Garden Grove, USA) and observed by microscopy using an Axiovert 200 microscope (Zeiss, Göttingen, Germany) equipped with a Tungsten lamp and a Mercury discharge lamp. Observations were done using 10×, 20×, and 40× A-Plan LD objectives (Zeiss, Göttingen, Germany). The photos were taken using a cooled Retiga 1300C color CCD camera (QImaging, Burnaby, Canada) and processed with Openlab version 3.1.7 software (Improvision, Coventry, UK).

For Nile Red microscopy, 1.5 µl of Nile Red stock solution (100 µM in ethanol) was added to 50 µl sample and aliquots were immediately measured. The final Nile Red concentration in the tested solutions was 3 µM. For Nile Red fluorescence, a Zeiss filter cube no. 15 was used (EX BP 546/12, BS FT 580, EM LP 590) additionally to the already described materials.

2.11. Evaluation of Trp-PEGs' hemocompatibility cytotoxicity

The cell proliferation kit II (XTT assay) from Roche Diagnostics (Basel, Switzerland) was used to determine the potential cytotoxicity of the two polymers on HaCaT cells (immortalized human keratinocyte cell line). Concentrations between 0.1 µg/ml and 20 mg/ml were tested. Defined numbers of 8×10^3 washed viable cells per well were incubated with serial dilutions of the polymers in 96-well plates (Nunclon TM Δ Surface by Nunc, Roskilde, Denmark) for a total of 24 and 48 h. Absorption at 490 nm was measured after 1, 3, 6, and 24 h by using a BioTek PowerWave XS reader (Witec AG, Littau, Switzerland). As a positive control for cytotoxicity, a 0.02% solution of SDS (sodium dodecyl sulfate) was used. Cells incubated with medium only served as the negative control. Calculated cell survival was normalized against the negative control. All measurements were performed in quadruplicate.

2.12. Evaluation of Trp-PEGs' hemocompatibility

The same concentrations of the compounds tested in the cytotoxicity assay were used to assess the potential of hemolysis due to membrane interactions and membrane lysis. After preparation of serial dilutions of polymers in sterile 0.9% NaCl, full human blood of a fasted volunteer (collected in citrate tubes) was added to the samples at a 1:3 (v/v) ratio. The positive control consisted of a 1% Triton X-100 solution and the negative control of 0.9% sterile NaCl. All the samples were put into an incubator at 37 °C for 1 and 24 h under shaking. After centrifugation (10 min at 770*g*), 40 µl of the supernatant were diluted four times with sterile 0.9% NaCl. After pipetting into a 96-well Costar® microplate (Product Number 3635, Corning Life Sciences, Schiphol, The Netherlands), the absorbance of released hemoglobin was measured at 575 nm employing a Tecan Safire microplate reader (Tecan Group Ltd., Männedorf, Switzerland). All measurements were performed in triplicates.

3. Results

3.1. Synthesis and characterization of the p-nitrophenyl carbonate mPEGs and Trp-mPEGs

The successful activation by *p*-nitrophenyl chloroformate and the successful conjugation of tryptophan to the mPEGs of 2 and 5 kDa molecular weight were analyzed by ^{1}H NMR, ^{13}C NMR, FTIR, MALDI-TOF and UV (see Sections 2.3–2.6 of synthesis of the different p-nitrophenyl mPEGs and Trp-mPEGs in Section 2). ^{1}H NMR indicated complete activation of mPEG-OH by *p*-nitrophenyl chloroformate, since the triplet at 4.56 ppm originating from the

hydroxyl group of mPEG-OH was no longer detected [26]. After the conjugation of L-Trp to *p*-nitrophenylcarbonate-mPEG, FTIR spectra revealed a shift of the ketone peak at ~1769 cm^{-1} to ~1721 cm^{-1}, indicating the successful conjugation of Trp (see Sections 2.3–2.6 of synthesis of the different p-nitrophenyl mPEGs and Trp-mPEGs in Section 2). MALDI-TOF indicated an increase in molecular weight as expected for *p*-nitrophenyl carbonate mPEG 2 kDa (pnp-PEG 2 kDa) and Trp-PEG 2 kDa (Table 2). pnp-PEG 5 kDa and Trp-PEG 5 kDa represented a molecular mass below the one of non-conjugated mPEG-OH. This may result from the purification process during the pnp-mPEG 5 kDa synthesis. The increase in molecular weight observed from pnp-mPEG 5 kDa to Trp-mPEG 5 kDa was again as expected. The degree of conjugation of Trp to PEG was determined by UV spectroscopy as an orthogonal method to ^{1}H NMR. Hence, impurities and excess L-Trp remaining from the synthesis can be excluded. A degree of conjugation of 98% was determined by UV spectroscopy for both Trp-mPEGs of 2 and 5 kDa molecular weight, while ^{1}H NMR again did no longer show the —OH triplet from mPEG-OH at 4.56 ppm or peaks from *p*-nitrophenol. Measurements of the specific optical rotation showed that a racemization of the chiral C-atom of L-Trp occurred on successful conjugation to mPEG.

3.2. Sensitivity of tryptophan-mPEGs to solvent polarity

Fig. 1A and C shows a blueshift of the fluorescence maximum with increasing ethanol concentration for Trp-mPEG 2 kDa (from 357 nm in water to 343 nm in 100% ethanol). The fluorescence intensity of the 2 kDa Trp-mPEG polymer first increased from water to 25% ethanol concentration, then constantly decreased from 25% to 100% ethanol concentration (Fig. 1A and B). A similar shift in fluorescence maximum and change of fluorescence intensity were observed for the Trp-mPEG 5 kDa (Fig. 1B and C).

3.3. Studies of potential of self-association of tryptophan-PEGs

Self-association of the Trp-mPEGs was tested by measuring the changes in the intrinsic Trp fluorescence depending on concentration using the Trp sensitivity toward solvent polarity. An increase in fluorescence intensity accompanied by a possible blueshift of the emission maximum might be observed when Trp is included into a more hydrophobic environment, e.g., a micellar core. The dependency of fluorescence intensity on the concentration of Trp-mPEG 2 kDa up to 1 mg/ml is shown in Fig. 2A. Low concentrations tested are enlarged in the insert where a small kink was measured at 0.0009 mg/ml (Fig. 2A). Up to 0.08 mg/ml linearity in the fluorescence versus concentration was observed. Fluorescence quenching of Trp occurred for concentrations between 0.08 mg/ml and 1 mg/ml. Therefore, different concentrations of the two Trp-mPEGs were analyzed by dynamic light scattering (DLS) to test for formation of large micelles. For Trp-mPEG 2 kDa, a linear increase in the intensity of scattered light as a function of concentration was obtained for concentrations of up to 20 mg/ml (Fig. 2B). Calculation of the mean hydrodynamic radii R_h (according to number distribution) for the different concentrations of Trp-mPEG 2 kDa resulted in values between 1.0 and 1.5 nm. For Trp-mPEG 5 kDa, a linear increase in the intensity of scattered light as a function of concentration was observed, as well (Fig. 2C). The calculated mean hydrodynamic radii R_h remained stable for all concentrations at a value of around 1.5 nm. As a control, the critical micelle concentration (CMC) of Tween 20® in water was correctly detected by DLS measurements (data not shown).

Table 2
Masses of the used mPEG-OHs and the resulting Trp-PEGs measured by MALDI-TOF mass spectrometry.

Compound	Observed *m*/*z* (M^+)
mPEG-OH 2 kDa	2080
p-Nitrophenyl carbonate-mPEG 2 kDa	2201
Trp-mPEG 2 kDa	2266
mPEG-OH 5 kDa	4839
p-Nitrophenyl carbonate-mPEG 5 kDa	4698
Trp-mPEG 5 kDa	4772

3.4. High throughput spectroscopic analysis

Nile Red fluorescence intensity at 620 nm and turbidity at 500 nm over time were measured for sCT and mixtures of different molar ratios of sCT and Trp-mPEG 2 kDa in 10 mM sodium citrate buffer, pH 6. Reduced turbidity and Nile Red fluorescence intensity were observed for the various samples in the following order: (i) sCT; (ii) sCT:Trp-mPEG 2 kDa = 1:1 and (iii) sCT:Trp-mPEG 2 kDa = 1:5; (iv) sCT:Trp-mPEG 2 kDa = 1:10. With increasing amounts of Trp-mPEG 2 kDa, the lag phase of sCT aggregation was prolonged (Fig. 3A and B). Increasing lag phases were measured in the following order: (i) sCT; (ii) sCT:Trp-mPEG 2 kDa = 1:1 and (iii) sCT:Trp-mPEG 2 kDa = 1:5; (iv) sCT:Trp-mPEG 2 kDa = 1:10. The Nile Red fluorescence intensity remained low and did not change for up to 64 h for the sample (Trp-mPEG 2 kDa concentration is 18.59 mg/ml). After 64 h, a small increase in Nile Red fluorescence intensity was observed. Turbidity for this solution did not change during the 74 h of the experiment although an increased absorbance of ~0.1 at 500 nm was observed directly at the beginning of the kinetics. The control solution containing 18.59 mg/ml Trp-mPEG 2 kDa showed a similar absorbance.

The influence of Trp-mPEG 5 kDa on the aggregation of sCT was studied. The Nile Red fluorescence intensity at 620 nm and turbidity at 500 nm over time of sCT and mixtures of sCT with of Trp-mPEG 5 kDa at various molar ratios in 10 mM sodium citrate buffer, pH 6, were measured (Fig. 4A and B). Up to ~25 h, turbidity remained similar for all samples tested (Fig. 4B). After 25 h, a decrease in turbidity in the following order was observed: (i) sCT; (ii) sCT:Trp-mPEG 5 kDa = 1:1; and (iii) sCT:Trp-mPEG 5 kDa = 1:5. Nile Red fluorescence over time during the 74 h of experiment was similar for sCT and the mixture of sCT and Trp-mPEG 5 kDa at a 1:1 ratio, although turbidity at 500 nm after 74 h was reduced for this mixture compared to sCT alone (Fig. 4A and B). The slope of the Nile Red fluorescence curve of the mixture of sCT and Trp-mPEG 5 kDa at a ratio of 1:5 was less pronounced compared to sCT and sCT:Trp-mPEG 5 kDa = 1:1. A plateau was reached for sCT:Trp-mPEG 5 kDa = 1:5 after about 17 h (Fig. 4A). The aggregation after 74 h for this solution was reduced compared to sCT alone and sCT:Trp-mPEG 5 kDa = 1:1, as observed by Nile Red fluorescence and turbidity measurements (Fig. 4A and B).

3.5. Interaction of Trp-mPEG 2 kDa with salmon calcitonin (sCT) at different molar ratios in 10 mM sodium citrate buffer, pH 5

No significant changes over time were seen in the fluorescence emission intensity of Tyr at 314 nm for the sCT sample in 10 mM sodium citrate buffer, pH 5. The tyrosine anisotropy remained constant during the aggregation of the sCT solution in 10 mM sodium citrate buffer, pH 5 (data not shown). Over time, a small increase in tyrosine lifetime was observed for this sample (Table 3). The 90° light scatter of sCT at 48 h showed only a small increase (data not shown), but was significantly increased after 72 h and increased further up to 216 h (Table 3). The UV–Vis absorbance of sCT at 500 nm slightly decreased after 24 h and then steadily increased up to 216 h (Table 3). Aggregates were observed for sCT after 48 h by fluorescence microscopy with Nile Red staining (Fig. 5G). The aggregation continued to increase for sCT as seen

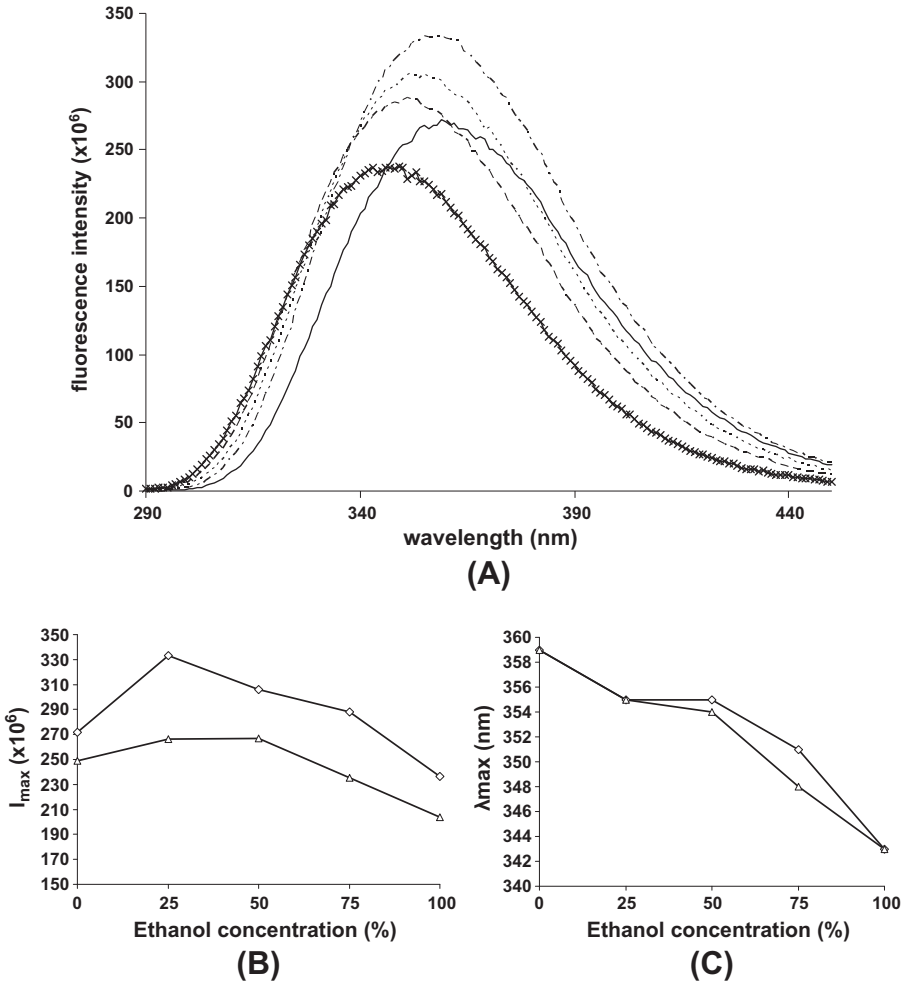

Fig. 1. Fluorescence dependency of Trp-mPEGs on different concentrations of ethanol. (A) Fluorescence emission spectra of Trp-mPEG 2 kDa. ––– fluorescence emission spectrum water; — • — fluorescence emission spectrum 25% ethanol; – – – fluorescence emission spectrum 50% ethanol; — — — fluorescence emission spectrum 75% ethanol; –×– fluorescence emission spectrum 100% ethanol. (B) Fluorescence intensity at the respective maxima against ethanol concentration (%) of the different Trp-PEGs. –◇– Trp-mPEG 2 kDa; –△– Trp-mPEG 5 kDa. (C) Wavelength of the fluorescence maxima against ethanol concentration (%) of the different Trp-PEGs. –◇– Trp-mPEG 2 kDa; –△– Trp-mPEG 5 kDa.

by the Nile Red photomicrographs from 72 and 216 h (Fig. 5J and M) and resulted in a strongly aggregated sample after 216 h (Fig. 5M). Significant increase in Nile Red fluorescence emission and a blueshift of its emission maximum were detected for this sample after 72 h (Table 4).

When Nile Red fluorescence intensity is too low ($<2.5 \times 10^6$), neither Nile Red anisotropy nor mean fluorescence lifetime can be measured (e.g., for 0–48 h of sCT). With the significant increase in Nile Red fluorescence intensity after 72 h, anisotropy and mean fluorescence lifetime of Nile Red could be measured. Both parameters increased from 72 h to 216 h (Table 4).

The fluorescence intensity of Trp in the sCT:Trp-mPEG 2 kDa = 1:1 sample decreased from 0 to 72 h and increased at 216 h. The lifetime of Trp in this mixture was stable for up to 48 h, then slightly increased up to the 216-h timepoint (Table 3). The Nile Red fluorescence emission at 630 nm for this solution slowly increased up to 72 h, but was too low to measure Nile Red anisotropy and mean fluorescence lifetime (Table 4). After 216 h, a strong increase in Nile Red fluorescence emission at 630 nm was detected. The Nile Red anisotropy for sCT:Trp-mPEG 2 kDa = 1:1 at 216 h was comparable to the value obtained for sCT after 216 h, while the mean fluorescence lifetime of Nile Red after 216 h was lower compared to sCT (Table 4). After 216 h, the Nile Red fluorescence emission intensity at 630 nm, the 90° light scatter, and UV–Vis absorbance at 500 nm for the mixture of sCT:Trp-mPEG 2 kDa = 1:1 were lower than for sCT alone (Fig. 6A and B, Tables 3 and 4). Nile Red microscopy showed some aggregates after 48 h for sCT:Trp-mPEG 2 kDa = 1:1 (Fig. 5H). After 72 h, the amount of aggregates for sCT:Trp-mPEG 2 kDa = 1:1 (Fig. 5K) was much smaller compared to sCT alone (Fig. 5J). Strong aggregation was observed for sCT:Trp-mPEG 2 kDa = 1:1 after 216 h by Nile Red microscopy (Fig. 5N).

After 24 h, a small increase in Trp fluorescence intensity was observed for sCT:Trp-mPEG 2 kDa = 1:10, which then constantly decreased up to 216 h (Table 3). The 90° light scatter of this sample was stable until 48 h, then increased after 72 h and further increased after 216 h. The 90° light scatter of sCT:Trp-mPEG 2 kDa = 1:10 at 216 h was significantly lower than the values measured at this time point for sCT alone and sCT:Trp-mPEG 2 kDa = 1:1 (Fig. 6A). The UV–Vis absorbance of sCT:Trp-mPEG 2 kDa = 1:10 at 500 nm decreased between 0 and 24 h, then remained stable until 72 h, and increased slightly after 216 h (Table 3). The mean Trp lifetime of the mixture of sCT:Trp-mPEG 2 kDa = 1:10 decreased after 24 h, then remained 7.25 ns up to 72 h, and decreased again after 216 h (Table 3). The Nile Red fluorescence for this sample slightly increased after 24 h, decreased again after 72 h, and remained stable until 216 h (Table 4). The Nile Red fluorescence intensity after 216 h was the smallest for (i)

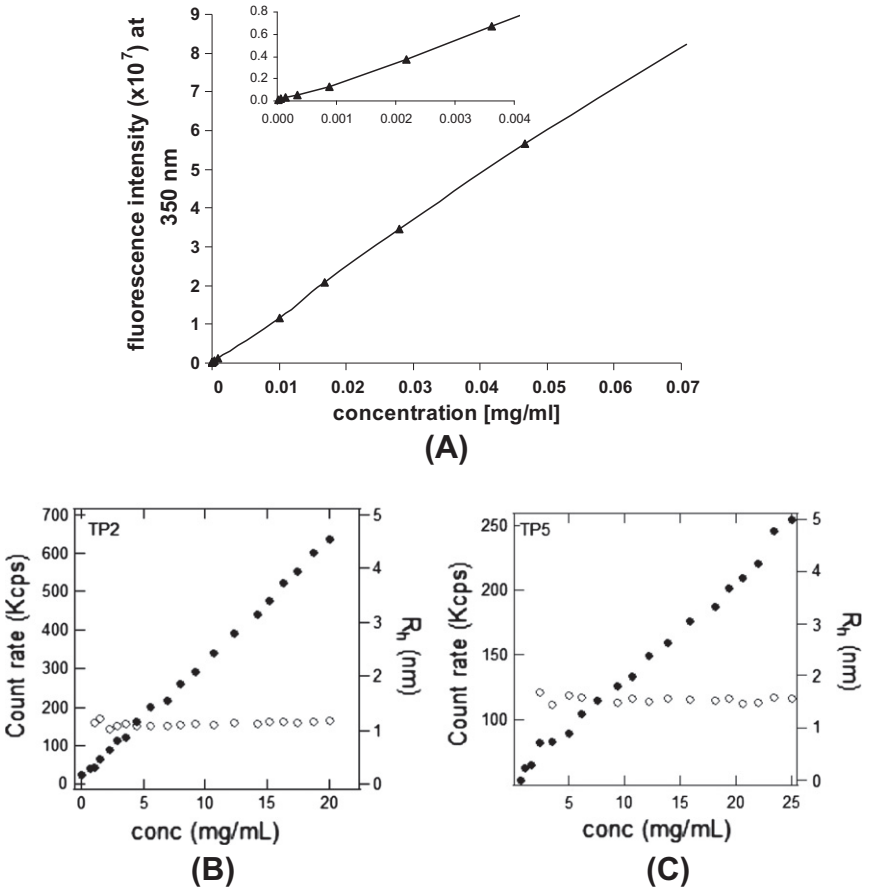

Fig. 2. (A) Fluorescence intensity of fluorescence maximum at 350 nm versus concentration of Trp-mPEG 2 kDa. (B) Dynamic light scattering (DLS) measured at an angle of 173°: Intensity of scattered light and hydrodynamic radius (R_h) at various concentrations of Trp-mPEG 2 kDa. (C) Dynamic light scattering (DLS) measured at an angle of 173°: Intensity of scattered light and hydrodynamic radius (R_h) at various concentrations of Trp-mPEG 5 kDa.

sCT:Trp-mPEG 2 kDa = 1:10, followed by (ii) sCT:Trp-mPEG 2 kDa = 1:1, and then by (iii) sCT (Fig. 6B). The Nile Red fluorescence emission up to 216 h of the sCT:Trp-mPEG 2 kDa = 1:10 mixture was very low, and therefore, neither Nile Red anisotropy nor the mean Nile Red lifetime could be measured (Table 4). Nile Red fluorescence microscopy did not detect any aggregates up to 216 h (Fig. 5C, F, I, L, and O).

3.6. Evaluation of Trp-mPEGs' cytotoxicity

A concentration of 20 mg/ml Trp-mPEG 2 kDa was cytotoxic after 48 h of incubation with HaCaT cells (Fig. 7). All other concentrations of Trp-mPEG 2 kDa down to 0.0001 mg/ml and all concentrations of Trp-mPEG 5 kDa (20 mg/ml included) were non-toxic after 48 h. The same results were observed after 24 h (data not shown).

3.7. Evaluation of Trp-mPEGs' hemocompatibility

All solutions of Trp-mPEG 2 kDa and 5 kDa were hemocompatible. None of the tested solutions did lyse erythrocytes after a maximum of 24 h of incubation with full human blood (Table 5).

4. Discussion

In this study, we investigated the potential of Trp-mPEGs of 2 and 5 kDa to reduce the aggregation of sCT. Tryptophan (Trp), tyrosine (Tyr), and phenylalanine (Phe) are aromatic amino acids that possess an intrinsic fluorescence. Out of these three, Trp has the strongest molar extinction coefficient and its fluorescence spectrum depends on its local environment. Therefore, it is often used as an intrinsic fluorescence probe to study protein conformation and intermolecular interactions [27,28]. Besides its hydrophobic nature, the fluorescence characteristics of Trp were further important reasons to evaluate Trp as a hydrophobic headgroup for our concept of non-covalent PEGylation. Furthermore, Trp is used as a nutritional supplement, and its maximum recommended therapeutic dose in humans is 100 mg/kg bodyweight/day [21].

The sensitivity of Trp-mPEGs to changes in the polarity of the environment was analyzed. As expected, with decreasing solvent polarity, a blueshift of the emission maximum occurred for both Trp-mPEGs (Fig. 1A and C) [25]. Changing from water to 25% ethanol solution caused an increase in fluorescence intensity, which may be explained by a reduced water quenching (Fig. 1A and B) [29]. Increasing the ethanol concentration from 25% to 100%, a constant decrease in fluorescence intensity was observed. Since the photophysics of tryptophan and its underlying indole structure are complex, the exact reason for the observed decrease in fluorescence intensity is unknown. Several possible quenching mechanisms might apply, such as quenching by the carbamate bond between Trp and PEG, the free negatively charged carboxylate or resonance energy transfer among the Trp residues [25,28–30].

Potential self-association of the Trp-mPEGs at low concentration was analyzed by using the sensitivity of Trp to changes in environmental polarity (Fig. 2A). An increase in fluorescence

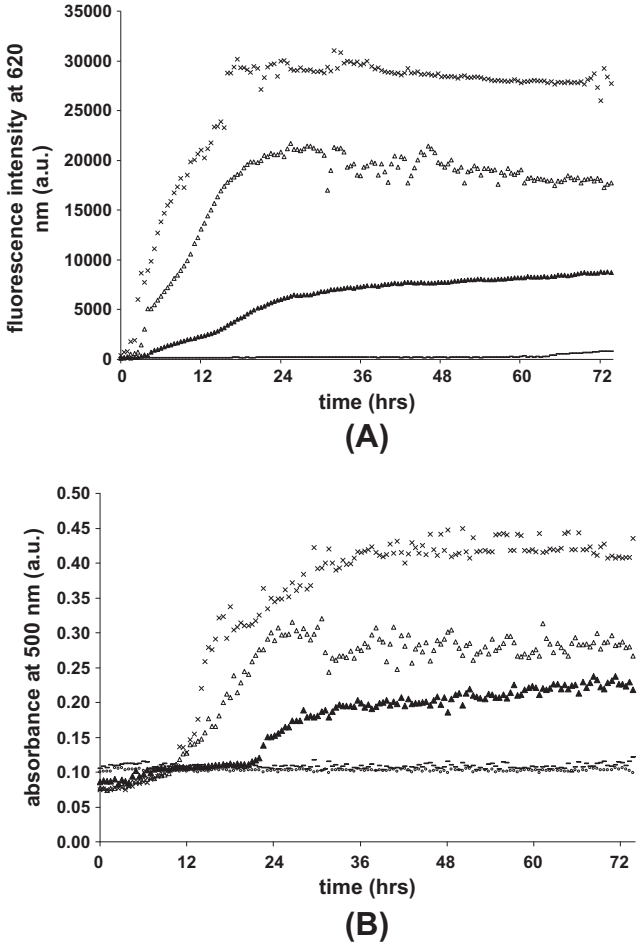

Fig. 3. Aggregation of salmon calcitonin in the presence of Trp-mPEG 2 kDa over time at different molar ratios. (A) Nile Red fluorescence at 620 nm in 10 mM sodium citrate buffer, pH 6. × salmon calcitonin; △ sCT:Trp-mPEG 2 kDa = 1:1; ▲ sCT:Trp-mPEG 2 kDa = 1:5; - - - sCT:Trp-mPEG 2 kDa = 1:10. (B) Turbidity at 500 nm in 10 mM sodium citrate buffer, pH 6. × salmon calcitonin; △ sCT:Trp-mPEG 2 kDa = 1:1; ▲ sCT:Trp-mPEG 2 kDa = 1:5; - - - sCT:Trp-mPEG 2 kDa = 1:10; Trp-mPEG 2 kDa 18.59 mg/ml.

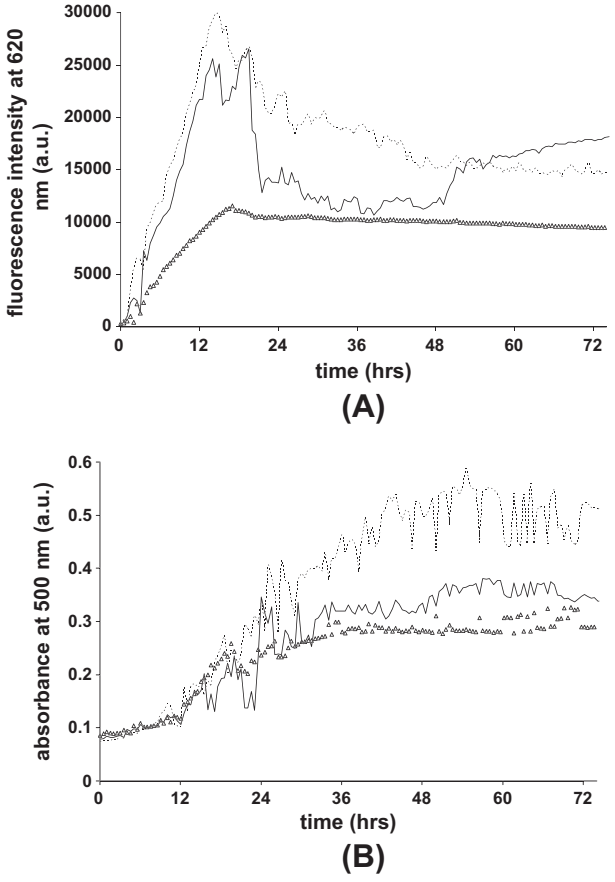

Fig. 4. Aggregation of salmon calcitonin in the presence of Trp-mPEG 5 kDa over time at different molar ratios in 10 mM sodium citrate buffer, pH 6. (A) Nile Red fluorescence at 620 nm in 10 mM sodium citrate buffer, pH 6. - - - salmon calcitonin; ––– sCT:Trp-mPEG 5 kDa = 1:1; △ sCT:Trp-mPEG 5 kDa = 1:5. (B) Turbidity at 500 nm in 10 mM sodium citrate buffer, pH 6. - - - salmon calcitonin; ––– sCT:Trp-mPEG 5 kDa = 1:1; Δ sCT:Trp-mPEG 5 kDa = 1:5.

intensity accompanied by a possible blueshift of the emission maximum might be observed when Trp is included into a more hydrophobic environment like a micellar core. Above 0.0009 mg/ml of Trp-mPEG 2 kDa, a steeper slope is observed in the curve showing the dependency of the fluorescence intensity on increasing concentration (Fig. 2A), which might indicate association of Trp-mPEG molecules. Quenching occurred for solutions with concentrations higher than 0.08 mg/ml (Fig. 2A). To test for association of larger molecular complexes, like micelles, solutions above 0.08 mg/ml were analyzed by dynamic light scattering (DLS). Formation of aggregates or micelles was not detected for any of the Trp-mPEGs by DLS, as can be seen by the linear increase in the intensity of scattered light/count rates with concentration (Fig. 2B and C). The hydrodynamic radii measured were ranging between 1 and 2 nm, similar to reported values in the literature [31], further indicating the absence of large complexes or micelles.

Hydrophobic fluorophores such as Nile Red possess a weak fluorescence in aqueous solutions. Being dissolved in apolar solvents or bound to hydrophobic surfaces, the fluorescence of Nile Red is strongly increased. Therefore, the fluorophore is used to follow the aggregation of proteins [23,24,32,33] and for the detection of micelles [34]. Figs. 3 and 4 showed only a weak fluorescence of Nile Red at the beginning of the kinetics even in the presence of high concentrations of Trp-mPEGs. Since no significant Nile Red fluorescence at various Trp-mPEG concentrations was detected, rather an absence of large micelles or aggregates of Trp-mPEGs is indicated. Therefore, the observed changes in fluorescence intensity of Trp-mPEG 2 kDa at 0.0009 mg/ml might be due to the association of two or three Trp-mPEG molecules, forming complexes that are too small to include a Nile Red molecule.

Capelle et al. have shown that sCT strongly aggregates at room temperature in 10 mM sodium citrate buffer, pH 6 [23]. Aggregation of sCT at different molar ratios of Trp-mPEG 2 kDa was reduced with increasing concentrations of Trp-mPEG 2 kDa as shown by changes in Nile Red fluorescence and turbidity over time (Fig. 3A and B). With increasing Trp-mPEG 2 kDa concentrations, the slopes of the Nile Red fluorescence intensity over time got less, indicating a decreased aggregation velocity (Fig. 3A). Turbidity over time showed a prolongation in the onset of aggregation of sCT with increasing Trp-mPEG 2 kDa concentration (Fig. 3B). In the solution of sCT:Trp-mPEG 2 kDa = 1:10, a stable and low Nile Red fluorescence suggested the absence of aggregation up to 64 h, while the turbidity remained stable during all of the 74 h of the kinetics. The increased turbidity (∼0.1) of this mixture at time point 0 of the kinetics can be assigned to the high concentration of Trp-mPEG 2 kDa. The reduction in sCT aggregation was also concentration dependent for Trp-mPEG 5 kDa, though to a lesser extent than for Trp-mPEG 2 kDa (Fig. 4A and B). Fig. 4B indicates a reduction in aggregation velocity and in the final degree of aggregation with increasing concentration of Trp-mPEG 5 kDa. Changes

Table 3
Aggregation of salmon calcitonin with Trp-mPEG 2 kDa in time at different molar ratios in 10 mM sodium citrate buffer, pH 5. UV–Vis absorbance at 500 nm, 90°light scatter at 450 nm (LS), fluorescence maxima (I_{max}) measured after excitation at 280 nm, and mean fluorescence lifetimes $\overline{\tau}$ measured in the emission maximum during the kinetics of sCT, sCT:Trp-mPEG 2 kDa = 1:1, and sCT:Trp-mPEG 2 kDa = 1:10 at time points 0, 24, 72, and 216 h.

Sample	Time (h)	Absorbance (a.u.)	LS (cps $\times 10^6$)	I_{max} (a.u. $\times 10^6$)	Lifetime $\overline{\tau}$ (ns)
sCT	0	0.08	0.05	2.7	1.48
	24	0.03	0.05	3.0	1.50
	72	0.07	0.36	2.9	1.50
	216	0.17	2.80	3.1	1.52
sCT:Trp-mPEG 2 kDa = 1:1	0	0.04	0.07	57	7.91
	24	0.07	0.06	55	7.91
	72	0.07	0.18	48	7.94
	216	0.13	1.74	50	7.96
sCT:Trp-mPEG 2 kDa = 1:10	0	0.16	0.23	63	7.36
	24	0.06	0.23	65	7.23
	72	0.06	0.28	54	7.27
	216	0.09	0.50	44	7.10

in Nile Red fluorescence over time did not reveal differences between the aggregation of sCT and sCT:Trp-mPEG 5 kDa = 1:1 as clear as turbidity (Fig. 4A and B). For the mixture of sCT:Trp-mPEG 5 kDa = 1:5, the highest value of Nile Red fluorescence was already reached after 17 h, as compared to 25 h observed by turbidity measurements. However, a reduction in aggregation velocity and in the final degree of aggregation was observed by both methods for sCT:Trp-mPEG 5 kDa = 1:5. For both Trp-mPEG polymers, aggregation of sCT was decreased in a harsh environment, where sCT rapidly aggregates. This stabilization was also visible by eye: the wells containing sCT:Trp-mPEG 2 kDa = 1:10 were clear while those containing sCT solution were turbid. In our studies, Trp-mPEG 2 kDa was superior to dansyl-mPEG 2 kDa in stabilizing sCT against aggregation. Though aggregation of sCT was reduced with dansyl-mPEG 2 kDa, no suppression of aggregation was obtained as was the case for Trp-mPEG 2 kDa in a 10-fold molar excess over sCT. The headgroup used appears to be important for inhibiting sCT aggregation.

The molecular weight of the used Trp-mPEG polymers also appears to have an effect on the observed reduction in sCT aggregation, as was also the case for the dansyl-PEGs. A significant reduction in aggregation of sCT was obtained with Trp-mPEG 2 kDa at a 1:1 molar ratio. A reduction in aggregation of sCT to a lesser extent was obtained with sCT:Trp-mPEG 5 kDa = 1:1. These results are comparable to observations made with the dansyl-PEGs and are contradictory to present covalent PEGylation, where preferably few and high molecular weight PEGs (e.g., 20 or 40 kDa) are employed [35]. Three possible explanations might apply: (i) the interaction of the Trp headgroup with sCT is reduced due to sterical hindrance caused by the PEG moiety, or (ii) with increasing molecular weight of the PEG the hydrophilic–lipophilic balance of Trp-mPEG is biased toward an increased influence of the PEG moiety on aggregation, which is detrimental for the interaction between the Trp headgroup and sCT [36], or (iii) with increasing molecular weight of the PEG the hydrophobic interactions between sCT and the dansyl-headgroup that allow sCT to remain in solution are decreased, and furthermore, increasing amounts of the solvation water from the outer shell of sCT are removed. As a result, sCT precipitates.

In our previous publication, we already presented that sCT:mPEG-OH 2 kDa = 1:1 in 10 mM sodium citrate buffer (pH 6) led to a similar aggregation as sCT in the absence of mPEG-OH. However, increasing aggregation of sCT was observed in equimolar mixtures with PEGs of increasing molecular weight. Similar observations were noticed during aggregation studies of Trp-PEGs (data not shown).

Changes in surface tension, viscosity, solvent polarity, and zeta potential of the protein might be induced by the addition of the excipients, leading to the effects described above. However, changes in surface tension can be excluded, since turbidity measurements have also been performed at 850 and 975 nm before and after the kinetic studies (data not shown). At these wavelengths, no absorbance of any of the compounds takes place, and therefore, variations in surface tension due to the addition of the excipients would have led to changes in the height and form of the solution meniscus. This in turn results into differences in the absorption signal in the multiwell plates. No differences in absorbance were observed between the various samples tested.

Furthermore, changes in solvent polarity due to the excipients can be excluded: Nile Red, the dye employed during our studies, is a fluorophore whose fluorescence intensity and also emission maximum are both susceptible to changes in environmental polarity. Since neither the situation of the emission maximum nor the emission intensity of Nile Red were different between the fluorescence spectra of sCT alone and sCT with increasing amounts of Trp-PEGs at T0, changes in environmental polarity due to our novel polymers can be excluded. However, small changes in viscosity or zeta potential of sCT due to the addition of Trp-PEGs cannot be excluded.

In 10 mM sodium citrate buffer, pH 5, sCT was reported to aggregate strongly [23]. Therefore, we investigated in this buffer system more profoundly the aggregation at different molar ratios of sCT:Trp-mPEG 2 kDa. Measurement of various parameters over time all showed consistently increasing aggregation of sCT (Tables 3 and 4 and Fig. 5A, D, G, J, and M). No changes were measured in the Tyr fluorescence emission and anisotropy, which suggested that aggregation did not directly involve Tyr. However, the increasing Tyr lifetime might indicate increasing conformational restrictions in the Tyr environment due to the aggregation.

Aggregation of sCT in the mixture of sCT:Trp-mPEG 2 kDa = 1:1 was already observed after 48 h, comparable to sCT without the excipient. However, 90° light scatter, UV–Vis absorbance, Nile Red fluorescence microscopy, Nile Red fluorescence emission, and mean lifetime of Nile Red indicated sCT was less aggregated in the presence of an equimolar amount of Trp-mPEG 2 kDa compared to sCT alone at time points 48, 72 and 216 h (Tables 3 and 4 and Figs. 6A, B and 5B, E, H, K, and N). Therefore, it can be concluded that Trp-mPEG 2 kDa at an equimolar amount stabilized sCT against aggregation.

The inhibition of sCT aggregation by Trp-mPEG 2 kDa is more pronounced at a molar ratio of sCT:Trp-mPEG 2 kDa 1:10. The 90° light scatter and Nile Red fluorescence emission were significantly reduced even after 216 h compared to sCT and sCT:Trp-mPEG 2 kDa at a 1:1 ratio (Fig. 6A and B). Nile Red fluorescence microscopy did not detect any aggregates up to 216 h (Fig. 5C, F, I, L, and O). UV–Vis absorbance at 500 nm is in agreement with the fluorescence and microscopy results (Table 3). For both solutions, sCT:Trp-mPEG 2 kDa = 1:1 and sCT:Trp-mPEG 2 kDa = 1:10,

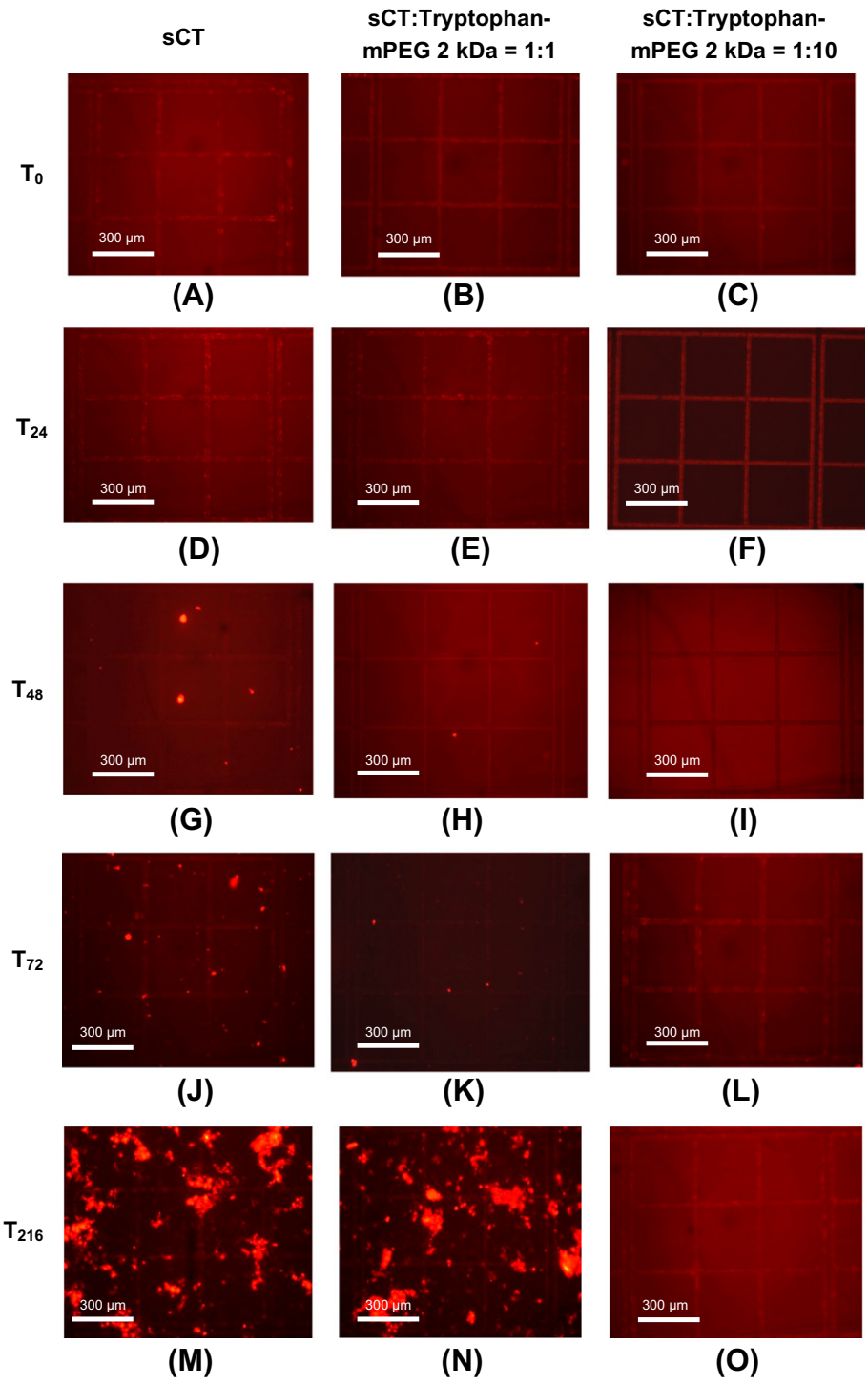

Fig. 5. Aggregation over time of salmon calcitonin in the presence of Trp-mPEG 2 kDa at different molar ratios in 10 mM sodium citrate buffer, pH 5, followed by Nile Red microscopy. Nile Red photomicrographs taken at time points 0, 48, 72 and 216 h during the aggregation of sCT, sCT:Trp-mPEG 2 kDa = 1:1, and sCT:Trp-mPEG 2 kDa = 1:10. Contrast and brightness of the photomicrographs were varied, to improve visibility of aggregates. (A) Time point 0: sCT 2.5 mg/ml. 11 s exposure time. (B) Time point 0: sCT:Trp-mPEG 2 kDa = 1:1. 4 s exposure time. (C) Time point 0: sCT:Trp-mPEG 2 kDa = 1:10. 5 s exposure time. (D) Time point 48 h: sCT 2.5 mg/ml. 6 s exposure time. (E) Time point 48 h: sCT:Trp-mPEG 2 kDa = 1:1. 5 s exposure time. (F) Time point 48 h: sCT:Trp-mPEG 2 kDa = 1:10. 3 s exposure time. (G) Time point 72 h: sCT 2.5 mg/ml. 7 s exposure time. (H) Time point 72 h: sCT:Trp-mPEG 2 kDa = 1:1. 5 s exposure time. (I) Time point 72 h: sCT:Trp-mPEG 2 kDa = 1:10. 10 s exposure time. (J) Time point 216 h: sCT 2.5 mg/ml. 4 s exposure time. (K) Time point 216 h: sCT:Trp-mPEG 2 kDa = 1:1. 3 s exposure time. (L) Time point 216 h: sCT:Trp-mPEG 2 kDa = 1:10. 8 s exposure time. (For interpretation of the references to color in this figure legend, the reader is referred to the web version of this article.)

a decrease in Trp fluorescence intensity was observed over time (Table 3). The sensitivity of the Trp emission to solvent polarity is affected by hydrogen bonding to the imino group and the surrounding electrical field of the solvent and solutes [25,37]. One explanation for the decrease in Trp fluorescence intensity of Trp-mPEG over time might be due to possible changes in hydrogen bonding or changes in the surrounding electrical field of the Trp-headgroup with progressing aggregation. However, increasing concentration of the Trp-mPEG 2 kDa might also be an influencing factor leading to increased resonance energy transfer.

Table 4
Aggregation of salmon calcitonin with Trp-mPEG 2 kDa in time at different molar ratios in 10 mM sodium citrate buffer, pH 5. Mean fluorescence lifetimes, anisotropy and fluorescence intensity at 630 nm of Nile Red measured for sCT, sCT:Trp-mPEG 2 kDa = 1:1, and sCT:Trp-mPEG 2 kDa = 1:10 at time points 0, 24, 72 and 216 h. N.d. refers to not detectable.

Sample	Time (hours)	Nile Red fluorescence intensity at 630 nm (a.u. $\times 10^6$)	Anisotropy of Nile Red (a.u.)	Mean lifetime $\bar{\tau}$ of Nile Red (ns)
sCT	0	0.59	n.d.	n.d.
	24	1.01	n.d.	n.d.
	72	2.79	0.31	3.48
	216	30.61	0.34	3.59
sCT:Trp-mPEG 2 kDa = 1:1	0	1.08	n.d.	n.d.
	24	1.13	n.d.	n.d.
	72	1.78	n.d.	n.d.
	216	19.22	0.35	3.51
sCT:Trp-mPEG 2 kDa = 1:10	0	1.42	n.d.	n.d.
	24	2.35	n.d.	n.d.
	72	1.83	n.d.	n.d.
	216	1.85	n.d.	n.d.

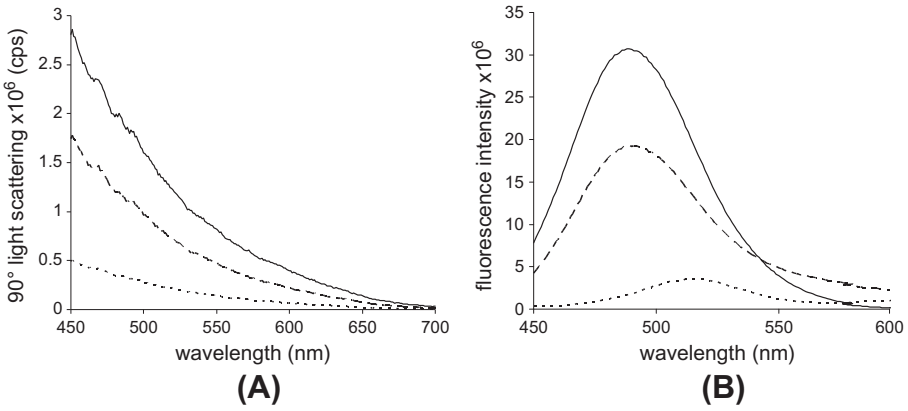

Fig. 6. Aggregation of salmon calcitonin in the presence of Trp-mPEG 2 kDa in time at different molar ratios in 10 mM sodium citrate buffer, pH 5. (A) 90° light scatter after 216 h in 10 mM sodium citrate buffer, pH 5. ––– salmon calcitonin; – – – sCT:Trp-mPEG 2 kDa = 1:1; - - - sCT:Trp-mPEG 2 kDa = 1:10. (B) Nile Red fluorescence emission after 216 h in 10 mM sodium citrate buffer, pH 5. ––– salmon calcitonin; – – – sCT:Trp-mPEG 2 kDa = 1:1; - - - sCT:Trp-mPEG 2 kDa = 1:10.

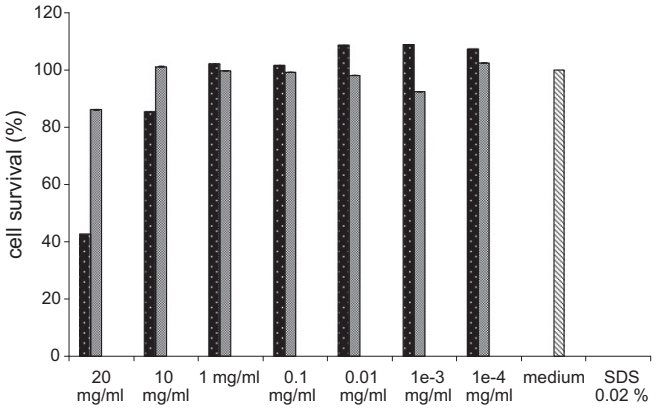

Fig. 7. Cytotoxicity of Trp-mPEGs tested on HaCaT cells after 48 h of incubation. Serial dilutions of Trp-mPEG 2 kDa, Trp-mPEG 5 kDa with positive (cells with 0.02% SDS) and negative control (cells with medium only).

Since the Trp-mPEGs are composed of a hydrophilic and a hydrophobic moiety, showing a detergent-like structure, destabilization of cellular membranes due to solubilization appears possible. To investigate the potential application of the Trp-PEGs as excipients for protein formulations, their cytotoxic and hemolytic activities were examined. Since proteins and peptides are often injected subcutaneously, immortalized keratinocytes were used to assess cytotoxicity.

After 48 h of incubation of various concentrations of the two Trp-mPEGs, only the solution of 20 mg/ml Trp-mPEG 2 kDa was cytotoxic (Fig. 7). The same concentrations of both Trp-mPEGs demonstrated no hemolytic properties in our assay (Table 5). Aggregation of biopharmaceuticals is dependent on concentration and elevated concentrations are known to increase aggregation [4,5]. A concentration of 2.5 mg/ml of sCT was used as a model for studying the inhibitory effect on the aggregation within a reasonable time span. In marketed formulations, the highest concentration of sCT is 0.37 mg/ml. Thus, toxic concentrations of

Table 5
Hemocompatibility of Trp-mPEGs. Different concentrations of Trp-mPEG 2 and 5 kDa were incubated for 24 h with full human blood. 0.9% NaCl and 1% Triton X-100 were taken as negative and positive control, respectively.

	20 mg/ml	10 mg/ml	1 mg/ml	0.1 mg/ml	0.01 mg/ml	0.001 mg/ml	0.0001 mg/ml	NaCl 0.9%	Triton X 1%
Trp-mPEG 2 kDa	100.12	100.47	100.35	100.81	100.27	100.61	100.72	100.00	0.00
Trp-mPEG 5 kDa	100.26	100.76	100.28	100.68	100.18	100.27	100.54		

20 mg/ml Trp-mPEG 2 kDa would not be clinically applied, if a 1:10 ratio of sCT:Trp-mPEG 2 kDa was maintained.

5. Conclusions

In this study, monofunctional Trp-PEGs of 2 and 5 kDa were synthesized and characterized by various techniques. These novel excipients reduced and suppressed the aggregation of sCT in different buffers dissolved in which sCT in the absence of excipients is unstable and prone to aggregation. Stabilization of sCT by Trp-mPEG 2 kDa was concentration dependent: with increasing Trp-mPEG 2 kDa concentration, sCT aggregation decreased. Trp-mPEG 5 kDa also stabilized sCT against aggregation in a concentration dependent manner in 10 mM sodium citrate buffer, pH 6, although to a minor extent than the 2 kDa Trp-mPEG. Trp-PEGs were non-hemolytic at all concentrations tested, while cytotoxicity was observed for Trp-mPEG 2 kDa at 20 mg/ml concentration.

Ongoing studies may reveal whether further properties of covalent PEGylation, such as reduced *in vivo* immunogenicity or improved pharmacokinetics, are maintained by our approach. Furthermore, a long-term study will investigate the effects of our novel Trp-PEGs on the stability of sCT under various accelerated aggregation conditions. Here, we presented novel excipients that can be easily prepared at low costs. Trp-mPEGs might be used for stabilizing aggregation prone and difficult to handle proteins as a promising alternative to current formulation strategies. With this approach, proteins might be formulated and marketed at higher concentrations, resulting in a more patient friendly and economic drug product.

Acknowledgements

The authors thank Prof. M. Borkovec, Department of Inorganic, Analytical, and Applied Chemistry of the University of Geneva, and his group for contributions to DLS measurements.

References

[1] S. Aggarwal, What's fueling the biotech engine-2007, Nat. Biotechnol. 26 (2008) 1227–1233.
[2] S. Lawrence, Billion dollar babies – biotech drugs as blockbusters, Nat. Biotechnol. 25 (2007) 380–382.
[3] G. Walsh, Biopharmaceuticals: recent approvals and likely directions, Trends Biotechnol. 23 (2005) 553–558.
[4] W. Wang, Protein aggregation and its inhibition in biopharmaceutics, Int. J. Pharm. 289 (2005) 1–30.
[5] H.C. Mahler, W. Friess, U. Grauschopf, S. Kiese, Protein aggregation: pathways, induction factors and analysis, J. Pharm. Sci. 98 (2009) 2909–2934.
[6] S.J. Shire, Formulation and manufacturability of biologics, Curr. Opin. Biotechnol. 20 (2009) 708–714.
[7] T.W. Randolph, J.F. Carpenter, Engineering challenges for protein formulations, Am. Inst. Chem. Eng. J. 53 (2007) 1902–1907.
[8] E.Y. Chi, S. Krishnan, T.W. Randolph, J.F. Carpenter, Physical stability of proteins in aqueous solution: mechanism and driving forces in nonnative protein aggregation, Pharm. Res. 20 (2003) 1325–1336.
[9] J.S. Philo, T. Arakawa, Mechanisms of protein aggregation, Curr. Pharm. Biotechnol. 10 (2009) 348–351.
[10] W. Wang, S. Nema, D. Teagarden, Protein aggregation – pathways and influencing factors, Int. J. Pharm. 390 (2010) 89–99.
[11] L. Runkel, W. Meier, R.B. Pepinsky, M. Karpusas, A. Whitty, K. Kimball, M. Brickelmaier, C. Muldowney, W. Jones, S.E. Goelz, Structural and functional differences between glycosylated and non-glycosylated forms of human interferon-beta (IFN-beta), Pharm. Res. 15 (1998) 641–649.
[12] A. Basu, K. Yang, M. Wang, S. Liu, R. Chintala, T. Palm, H. Zhao, P. Peng, D. Wu, Z. Zhang, J. Hua, M. Hsieh, J. Zhou, X. Petti, A. Janjua, M. Mendez, J. Liu, C. Longley, Z. Zhihua, M. Mehlig, V. Borowski, M. Viswanathan, D. Filpula, Structure–function engineering of interferon-β-1b for improving stability, solubility, potency, immunogenicity, and pharmacokinetic properties by site-selective mono-pegylation, Bioconjugate Chem. 17 (2006) 618–630.
[13] C. Dhalluin, A. Ross, L.A. Leuthold, S. Foser, B. Gsell, F. Müller, H. Senn, Structural and biophysical characterization of the 40 kDa PEG-interferon-α2a and its individual positional isomers, Bioconjugate Chem. 16 (2005) 504–517.
[14] R.S. Rajan, T. Li, M. Aras, C. Sloey, W. Sutherland, H. Arai, R. Briddell, O. Kinstler, A.M. Lueras, Y. Zhang, H. Yeghnazar, M. Treuheit, D.N. Brems, Modulation of protein aggregation by polyethylene glycol conjugation: GCSF as a case study, Protein Sci. 15 (2006) 1063–1075.
[15] P. Caliceti, F.M. Veronese, Pharmacokinetic and biodistribution properties of poly(ethylene glycol)–protein conjugates, Adv. Drug Deliv. Rev. 55 (2003) 1261–1277.
[16] M.L. Graham, Pegaspargase: a review of clinical studies, Adv. Drug Deliv. Rev. 55 (2003) 1293–1302.
[17] N.V. Katre, The conjugation of proteins with polyethylene glycol and other polymers. Altering properties of proteins to enhance their therapeutic potential, Adv. Drug Deliv. Rev. 10 (1993) 91–114.
[18] F.M. Veronese, G. Pasut, PEGylation: posttranslational bioengineering of protein biotherapeutics, Drug Discov. Today: Technol. 5 (2008) e57–e64.
[19] C. Mueller, M.A.H. Capelle, T. Arvinte, E. Seyrek, G. Borchard, Non-covalent PEGylation as a new means against aggregation of salmon calcitonin, J. Pharm. Sci. 100 (2011) 1648–1662.
[20] G. Borchard, C. Mueller, M.A.H. Capelle, T. Arvinte, Stabilized Protein Formulations and use thereof, Patent WO 2011/051916 A2, 2011.
[21] FDA. <http://www.fda.gov/AboutFDA/CentersOffices/CDER/ucm092199.htm#T> (accessed on 02.09.10).
[22] F. Veronese, Biologically active drug polymer derivatives and method for preparing same, Patent US005286637, 1994.
[23] M.A. Capelle, R. Gurny, T. Arvinte, A high throughput protein formulation platform: case study of salmon calcitonin, Pharm. Res. 26 (2009) 118–128.
[24] B. Demeule, M.J. Lawrence, A.F. Drake, R. Gurny, T. Arvinte, Characterization of protein aggregation: the case of a therapeutic immunoglobulin, Biochim. Biophys. Acta 1774 (2007) 146–153.
[25] J.R. Lakowicz, Protein fluorescence, in: J.R. Lakowicz (Ed.), Principles of Fluorescence Spectroscopy, Kluwer Academic/Plenum Publishers, New York, 2006.
[26] J.M. Dust, Z. Fang, J.M. Harris, Proton NMR characterization of poly(ethylene glycols) and derivatives, Macromolecules 23 (1990) 3742–3746.
[27] P.R. Callis, 1La and 1Lb transitions of tryptophan: applications of theory and experimental observations to fluorescence of proteins, in: L. Brand, M.L. Johnson (Eds.), Methods Enzymol., vol. 278, Academic Press, New York, 1997. pp. 113–150.
[28] Y. Chen, M.D. Barkley, Toward understanding tryptophan fluorescence in proteins, Biochemistry 37 (1998) 9976–9982.
[29] P.R. Callis, T. Liu, Quantitative prediction of fluorescence quantum yields for tryptophan in proteins, J. Phys. Chem. B 108 (2004) 4248–4259.
[30] Y. Chen, B. Liu, H.T. Yu, M.D. Barkley, The peptide bond quenches indole fluorescence, J. Am. Chem. Soc. 118 (1996) 9271–9278.
[31] H. Lee, R.M. Venable, A.D. Mackerell Jr., R.W. Pastor, Molecular dynamics studies of polyethylene oxide and polyethylene glycol: hydrodynamic radius and shape anisotropy, Biophys. J. 95 (2008) 1590–1599.
[32] A. Hawe, M. Sutter, W. Jiskoot, Extrinsic fluorescent dyes as tools for protein characterization, Pharm. Res. 25 (2008) 1487–1499.
[33] M. Sutter, S. Oliveira, N.N. Sanders, B. Lucas, A. van Hoek, M.A. Hink, A.J. Visser, S.C. De Smedt, W.E. Hennink, W. Jiskoot, Sensitive spectroscopic detection of large and denatured protein aggregates in solution by use of the fluorescent dye Nile Red, J. Fluorescence 17 (2007) 181–192.
[34] T. Trimaille, K. Mondon, R. Gurny, M. Moller, Novel polymeric micelles for hydrophobic drug delivery based on biodegradable poly(hexyl-substituted lactides), Int. J. Pharm. 319 (2006) 147–154.
[35] M.J. Roberts, M.D. Bentley, J.M. Harris, Chemistry for peptide and protein PEGylation, Adv. Drug Deliv. Rev. 54 (2002) 459–476.
[36] W. Griffin, Calculations of HLB values of nonionic surfactants, J. Soc. Cosmet. Chem. 5 (1954) 249–256.
[37] P.R. Callis, B.K. Burgess, Tryptophan fluorescence shifts in proteins from hybrid simulations: an electrostatic approach, J. Phys. Chem. B 101 (1997) 9429–9432.